INTERNATIONAL JOURNAL OF RESEARCH SCIENCE & MANAGEMENT

PHOTOCATALYTIC ACTIVES OF PVDF/TIO2 PRODUCED BY SOLUTION BLOW SPINNING WITH SILVER NANOPARTICLES ADSORBED ON THE SURFACE

G. S. Padovani; T. C. Gimenes; S. A. P. T. de Carvalho; A. O. Sanches: L. F. Malmonge; F. R. de Paula*.
Universidade Estadual Paulista (UNESP), Engineering University, Campus of Ilha Solteira, Ilha Solteira, SP, 15385-000, Brazil.

Abstract

An efficient method for manufacturing nano-submicron PVDF/TiO2 fibers was developed by solution blow spinning and subsequent incorporation of silver nanoparticles. In this work, we tried to use Ag particles prepared by the reduction of AgNO3 with NaBH4 in solution to increase the photocatalytic activity of the membrane; the nanoparticles remained on the surface of the PVDF/TiO2 fibers after the bath. The SEM image shows transparent fibers with Ag nanoparticles coated along the entire fiber. XRD revealed the anatase and rutile phases and the metallic form of Ag, and XPS confirmed Ti and O as well as Ag. In the presence of silver nanoparticles, fibers showed a significant increase in dye degradation, and excess silver was also observed to decrease photocatalytic activity. Furthermore, the fibers show promise as antibacterial agents.

Keywords: Photocatalytic membrane: titanium dioxide; nanocomposites; membranes, SBS method

Introduction

Due to the massive production of organic and inorganic pollutants caused by the development of modern society, the control and treatment of pollution have been the subject of extensive research. In the poorest countries, poor sanitation and the release of industrial waste into water and air lead to premature death, particularly among newborns and children. According to the World Health Organization (WHO), 5.3 billion people drink biologically and chemically polluted water [1]. In this sense, photocatalytic semiconductors for water and air purification [2-5] have been widely studied, mainly because they are superior to other catalytic methods, such as complete waste mineralization, low cost, and working pressure at room temperature [6-8].

Although many semiconductor materials can be used as photocatalysts, they must possess crucial properties such as photoreactivity under sunlight, biologically and chemically inert, non-toxic when used in the environment, and photostable, i.e., they do not degrade during the process of photoreaction and should have a low production cost [9]. Titanium dioxide (TiO_2) has these properties and has been extensively studied in the last 30 years [10] to degrade organic molecules such as phenols, dyes, pesticides, and pharmaceuticals. [11–14]. Many studies have applied titanium dioxide to the environment. Haider et al. [15] prepared a thin TiO_2 layer as a self-cleaning coating for windows. Bel Hadjltaief et al. [16] investigated TiO_2/clay composites to treat dye Rhodamine B (RhB) in water; the composites exhibited high photocatalytic activity under UV light irradiation. Luo et al. [17] mixed TiO_2 and ZnO nanoparticles with cement and demonstrated antifungal activity by dye degradation and in vitro biodegradation. Even with myriad applications, using TiO_2 in the environment as a usable and practical form remains challenging. This is due to the disadvantage of TiO_2 because high electron-hole recombination, on the order of a few nanoseconds, stops the oxidation and reduction sites, resulting in reduced photocatalytic activity [18,19].

Recently, as a way to improve the disadvantages of TiO_2, such as the high electron-hole recombination, and consequently improve the photocatalytic performance, many noble metals such as Pt, Ag, Au, and Pd [20-26] were incorporated through different methods such as doping, impregnation, photo-reduction, etc. Combining these metals with TiO_2 can create a synergy that can reduce photogenerated electron-hole recombination, allowing the oxidizing and reducing sites to remain active for a longer time. Another consequence is modifying the absorption range of the photocatalyst from near UV to visible light [27,28]. This control over its physical properties and the existence of bactericidal activity has sparked interest in using TiO_2-Ag composites over the past few decades. Ashkarran et al. [34] prepared TiO_2-Ag nanoparticles and investigated their antibacterial activity against Escherichia coli under UV irradiation and visible light. Studies have shown that the bacterial action of pure TiO_2 is low, but the antibacterial activity of TiO_2-Ag composites is improved.

Due to the unique properties of silver nanoparticles, TiO_2-Ag exerts its antibacterial effect even in the absence of UV light. However, photogenerated hydroxyl radicals accelerate the oxidation process under UV irradiation, destroying bacteria and viruses more efficiently up to complete mineralization.

There are several obstacles to using TiO_2-Ag nanoparticles in environmental problems, one of which is the need for a complex structure to keep the particles in suspension. This work attempts to solve this problem by producing PVDF/TiO_2-Ag fibers by SBS technique without degrading the properties of interest. This method developed by Medeiros et al. [35] makes it possible to obtain fibers in a similar way to electrospinning [36-40], but using airflow and has the advantage of allowing fibers to be produced in less time, at a lower cost and in the way they are formed, they can be used for in situ application on skin lesions [41,42].

Experimental

2.1. Materials

Polyvinylidene fluoride (PVDF, Mw = 30,000 g/mol), silver nitrate ($AgNO_3$) and sodium borohydride ($NaBH_4$), and the dye Rhodamine B (RhB) was purchased from Sigma-Aldrich, Dioxide titanium (TiO_2) Degussa (P25) were obtained from Nippon Aerosil CO LTD. All reagents were used without purification.

2.2. Preparation of solution blow spinning PVDF/TiO_2 microfibers membranes

The PVDF polymer was dissolved in N,N-dimethylformamide (DMF) at a concentration of 20% by weight (w/v). The solution was stirred vigorously for one h at 70°C. After this time, TiO_2 nanoparticles were added to the solution in the proportion of 50% of the polymer mass and stirred at room temperature. The solution was transferred to a plastic syringe which was later inserted into the SBS equipment. The parameters used in producing the fibers were 76 µl/min for the feed rate, 400 rpm in the rotating collector, 21 cm between the needle tip and the collector, and the pressure used in the system was 140 kPa. The fiber membrane was collected in aluminum foil and then peeled.

2.3. Silver adsorption on the surface of PVDF/TiO_2 membranes

PVDF/TiO_2 fibers previously prepared by SBS technique were first immersed in $AgNO_3$(aq) solutions of different concentrations (14.7; 44.2; 58.9; 88.3; 117.8 mmol/l). After soaking for 5 minutes, the fibers were removed, and the NaBH-$_4$(aq) (mmol/l) solution was sprayed onto their surface and then dried at room temperature, as shown in Figure 01.

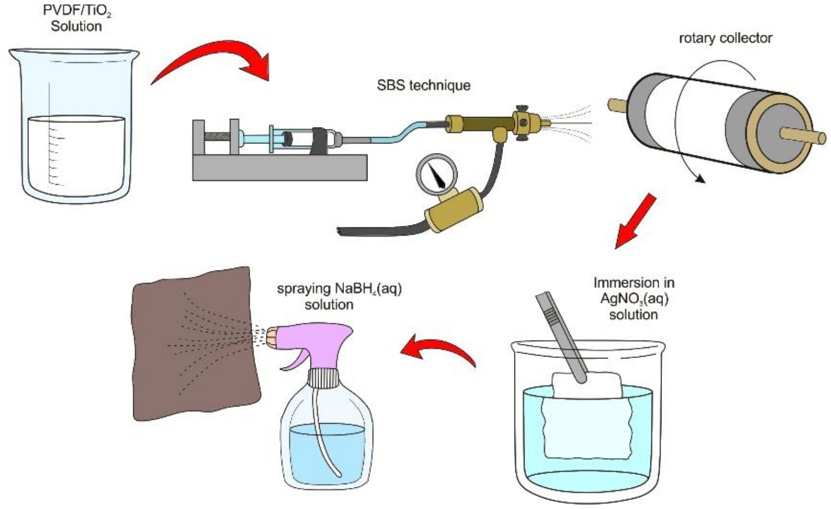

Figure 01: Schematic illustration of the preparation of PVDF/TiO_2-Ag membrane.

2.4 Characterization

The X-ray diffraction (XRD) technique was used to define the structure and phases of the samples. The equipment was a Shimadzu model, XRD-6000, CuKα ($\lambda = 1.54$ Å). The morphology and diameter of the fibers were obtained using scanning electron microscopy techniques. For this characterization, the Zeiss EVO LS15 model was used at 10 kV. The photocatalytic efficiency of the samples was evaluated using a Varian Cary 50 Scan brand UV-vis spectra.

2.5. Evaluation of photocatalytic activity

The photocatalytic activity of PVDF/TiO_2-Ag was evaluated by the degradation of RhB in an aqueous solution under UV irradiation. A closed box equipped with a 150 W mercury UV lamp located 25 cm from the sample was used for the photocatalytic test. To prepare the solution was added 0.02 mol/l RhB and 0.08 g PVDF/TiO_2-Ag fibers to 100 ml distilled water. With vigorous mechanical agitation, every 5 minutes under UV irradiation, 2 mL aliquots of the solution were removed for analysis in a UV-Vis spectrophotometer.

Results and Discussions

3.1 Structure and morphology of PVDF/TiO_2-Ag Membranes

First, before obtaining the PVDF/TiO_2_Ag fibers, the initial conditions for obtaining the most efficient PVDF/TiO_2 photocatalytic fibers were determined. After obtaining this parameter, silver nanoparticles were added to the fibers. The incorporation was performed by immersing the blanket in a solution containing $AgNO_3$, allowing the Ag+ ions to be adsorbed on the surface. The $NaBH_4$ solution was then sprayed onto the film where silver ion oxidation occurred. BH_4^- ions generate repulsive force to stabilize silver nanoparticles. The process of obtaining nanoparticles is shown in Figure 01.

Figure 02 shows the fibers obtained by the SBS technique after the removal of the collector. All parameters were kept constant during fiber production and extraction. The images of the PVDF/TiO_2 fibers show the presence of surface roughness and a mean diameter of approximately 629 nm. An increase in roughness was observed for fibers with Ag incorporation (Fig. 2b–f).

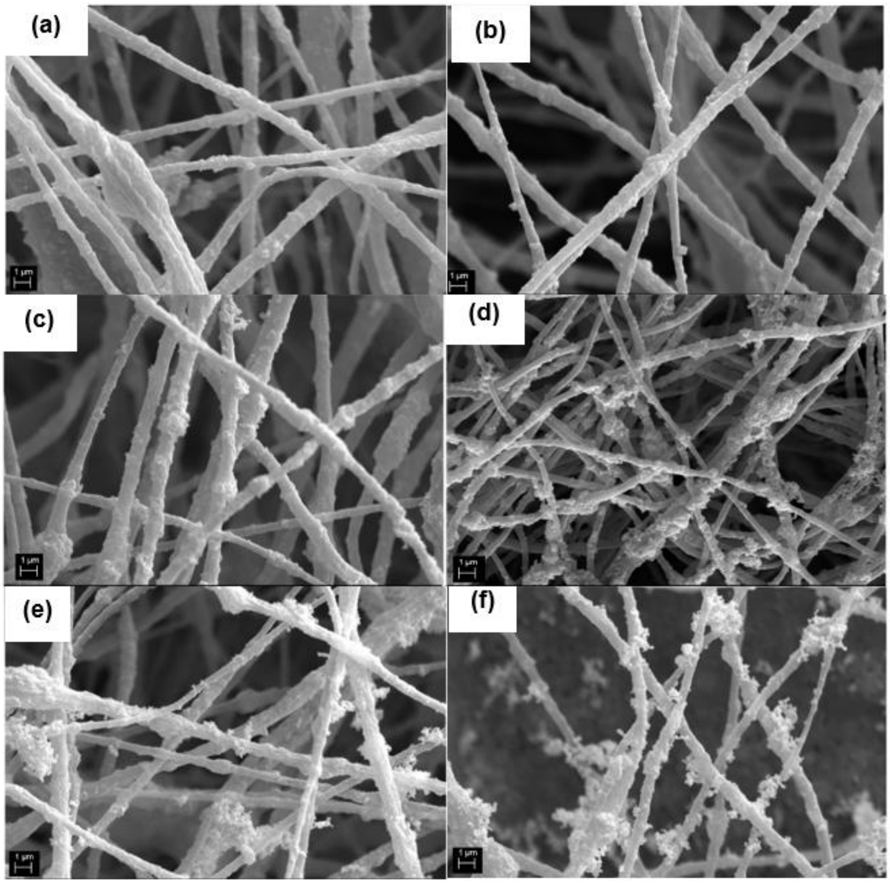

Figure 02. SEM images of PVDF/TiO_2 (a) Pure and with (b) 14.7 mmol/l (c) 44.2 mmol/l (d) mmol/l (e) 88.3 mmol/l (f) 117.8 mmol/l of $AgNO_3$ in immersion process.

The presence of TiO_2 and Ag nanoparticles was confirmed by XRD measurement. Figure 03 shows the XRD patterns of PVDF/TiO_2-Ag, where all membranes show similar peaks. Due to the high-pressure gas used in the SBS technique, the polymer's stretching during the solvent's evaporation causes the PVDF to pass from the alpha phase to the beta phase, which can be observed by the presence of the first peak at 20.5°. As expected, the most intense peaks, 25.2° (101); 48.1° (200), indicate the presence of the anatase phase and the presence of diffraction peaks 27.4° (110); 36.1° (101); 54.3° (221) the presence in all samples of the rutile phase. The silver-related peaks are visible only in the sample at 117.8 mmol/l. In contrast, in the other samples with lower concentrations, the characteristic peaks of silver are superimposed on those of the anatase phase. The hiding of the peaks occurs because silver is only on the membrane surface, and its concentration is low when compared to the presence of TiO_2.

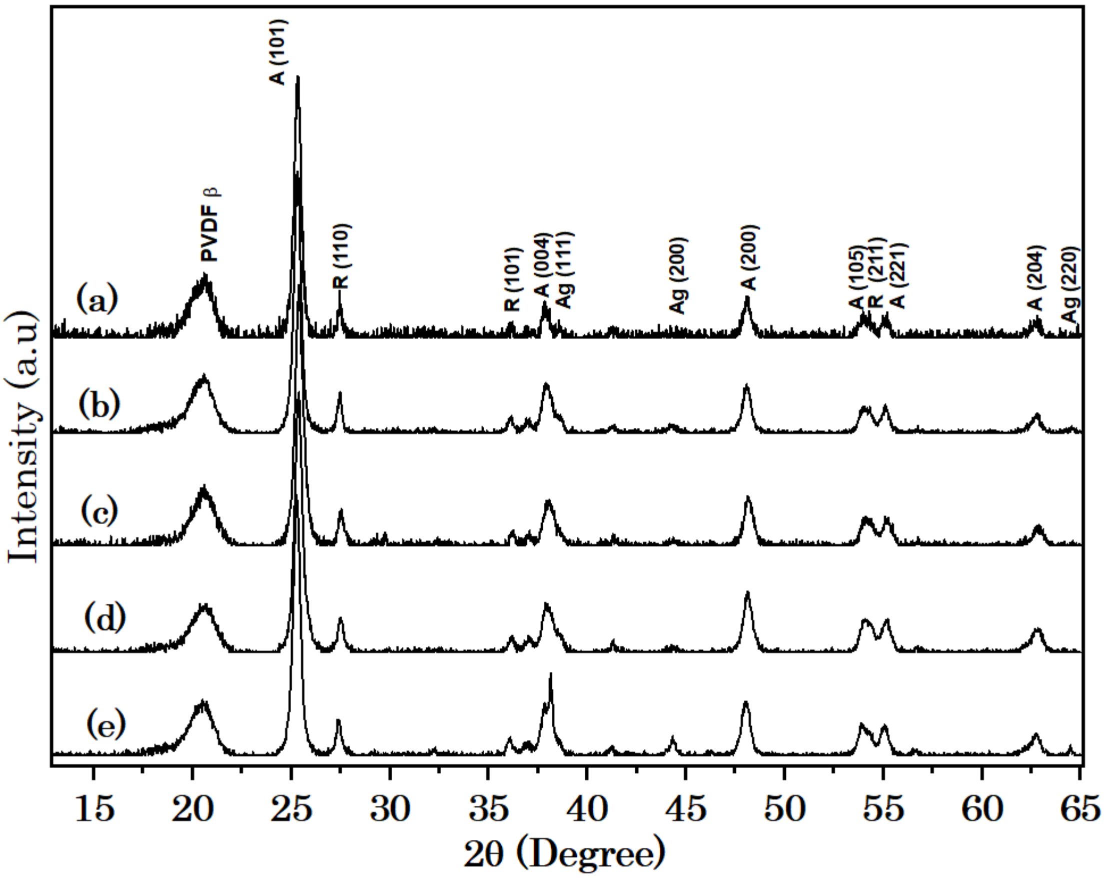

Figure 03: (a) XRD pattern of PVDF/TiO_2 membranes with different $AgNO_3$ concentrations used in immersion process: (a) 14.7 (b) 44.2, (c) 58.9, (d) 88.3, and (e) 117.8 mmol/l, respectively. (A-Anatase, R-Rutile, Ag- Silver).

As shown na Figure 04, the EDX spectra also confirmed the presence of TiO_2 and silver in the fibers. A strong Ti peak and a weaker O peak can be observed. Smaller Ag peaks were also observed. The results show that the content of each element is Ti=48.2%, O=46.9%, Ag=4.9%.

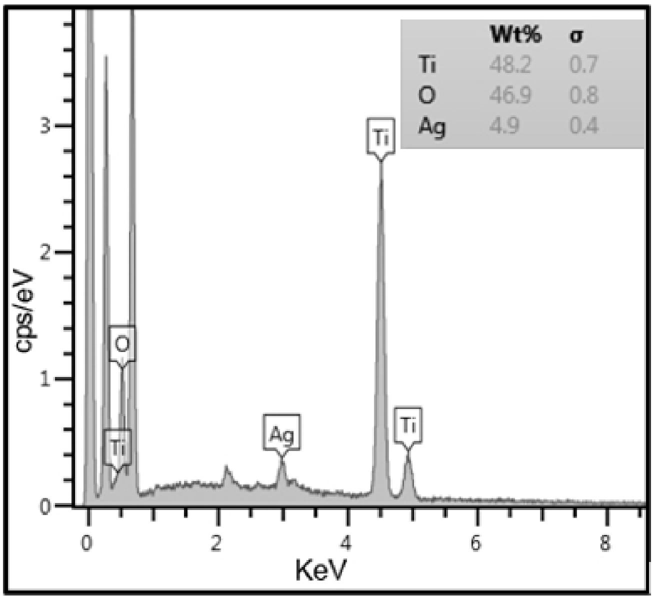

Figure 04. EDX spectra of membrane with immersion concentration of 58.9 mmol/l.

3.2 Photocatalytic performance of PVDF/TiO_2-Ag Membranes

Decolorizing RhB evaluated the photocatalytic performance of PVDF/TiO_2 and PVDF/TiO_2-Ag at room temperature; this organic dye was used for being considerate between the significant discharges from the textile industry. The photocatalytic oxidation of RhB was monitored by taking UV–vis measurements at various light exposure times. Before the photocatalytic assay, the samples were immersed in RhB solution and agitated for 10 minutes to ensure adsorption or absorption equilibrium.

The Uv-vis spectra were set between 450-610 nm, being the λmax of RhB dye at 540 nm. Figure 05 shows the effect of photocatalytic degradation using $\mathbf{C/C_0}$ versus time equation, where $\mathbf{C_0}$ is the initial concentration of RhB and **C** is the concentration of RhB that was degraded at time. In the absence of any catalyst, the RhB possesses a low degradation after 20 min. As expected, the PVDF/ TiO_2 membrane has a pronounced dye degradation, degrading 57% in the same period time the use of TiO_2 Degussa P25 in the fibers occurred for two reasons the ease of finding this semiconductor on the market and due to the synergy between the anatase and rutile phases having a better photocatalytic activity when compared to one of the two separate phases. After the membrane treatment with Ag, the fibers had considerably increased the photocatalytic process, the concentrations of 14.7, 44.2, and 58.9 mmol/l degraded approximately 64, 87, and 95 % after 20 min. of exposure UV irradiation. The catalytic activity of membranes increases and then decrease with the increase of the $AgNO_3$ concentration been; the optimum concentration was 58.9 mmol/l three-dimensional coating with silver on PVDF/TiO_2 fibers was necessary because the superficial interaction between Ag and TiO_2 generates an interface transfer charge. This phenomenon occurs when the TiO_2 absorbs photons of suitable energy greater or equal to his bandgap, the electrons are promoted to the conduction band (CB) and leave the same number of holes in the valence band (VB). It is supposed that the photoinduced electrons would transfer from TiO_2 to Ag particles. This separation of charges prevents recombination and consequently increases photocatalyst activity.

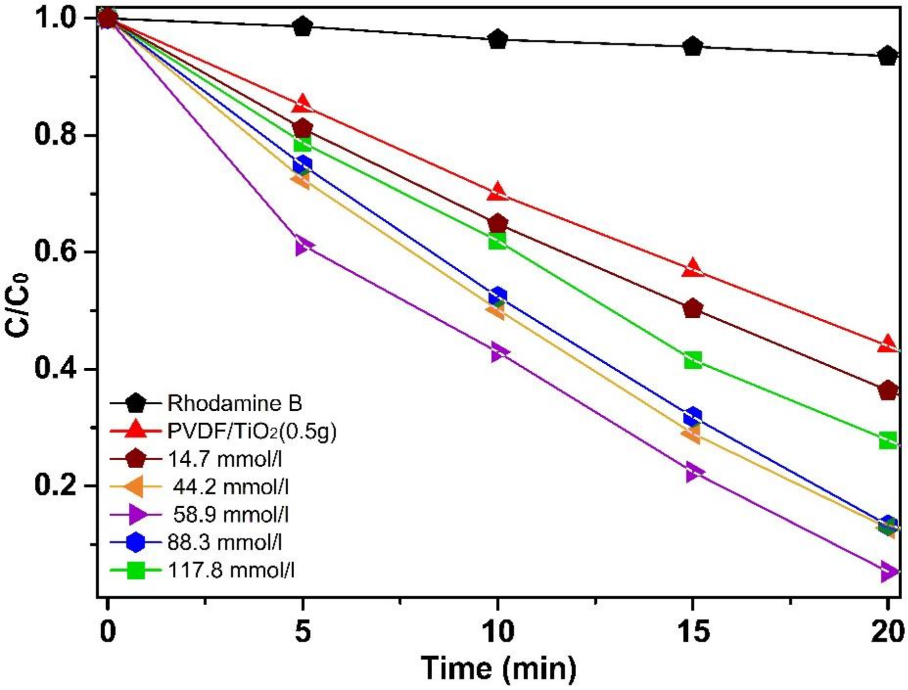

Figure 05. Photocatalytic degradation of RhB under UV irradiation.

Two factors could explain the decrease in the concentrations of 88.3 and 117.8 mmol/l, the increase in the size of the nanoparticles due to the high ionic tension of the medium when present in a solution of $NaBH_4$ which also leads to the increase and agglomeration of the particles increase the surface area of the particles agglomerated preventing the interaction of more particles with TiO_2. Therefore, there is no interaction and superficial electronic transfer between these two materials. This composite membrane enables photocatalyst filter and antibacterial applications due to high resistance, excellent flexibility, and stability. During photocatalytic tests, there was no detachment of particles in solution even under intense agitation, which would hinder or render infeasible some processes with only TiO_2/Ag particles.

Conclusion

In summary, PVDF/TiO_2 membranes were produced by the SBS technique, where the fibers showed a well-defined surface and an average diameter of 500 nm. The impregnation of Ag nanoparticles was facile synthesized by reducing $AgNO_3$ salt and remained attached to the membrane. The photocatalytic results showed that the membrane of PVDF/TiO_2 degraded approximately 50% of the dye, the high degradation of the membranes could be attributed to the nanoparticles of TiO_2, which contain a heterojunction between Anatase and Rutile. Moreover, the impregnation of Ag nanoparticles doubled the photocatalytic activity. The optimum concentration for impregnation was 58.9 mmol/L of $AgNO_3$, which can be attributed to the balance between fiber coating and the surface area. Therefore, PVDF/TiO_2-Ag membranes are promising due to their flexibility, large surface area, fiber resistance, and high photocatalytic activity, which is possible until future studies address their macrobiotic activity.

References

1. WHO & UNICEF. Progress on Drinking Water, Sanitation and Hygiene 2017. (2017).
2. Hoffmann, M. R., Martin, S. T., Choi, W. & Bahnemann, D. W. Environmental Applications of Semiconductor Photocatalysis. Chem. Rev. 95, 69–96 (1995).
3. Linsebigler, A. L., Lu, G. & Yates, J. T. Photocatalysis on TiO2 Surfaces: Principles, Mechanisms, and Selected Results. Chem. Rev. 95, 735–758 (1995).
4. Mills, A., Davies, R. H. & Worsley, D. Water purification by semiconductor photocatalysis. Chem. Soc. Rev. 22, 417–425 (1993).
5. Ochiai, T. & Fujishima, A. Photoelectrochemical properties of TiO2 photocatalyst and its applications for environmental purification. J. Photochem. Photobiol. C Photochem. Rev. 13, 247–262 (2012).

6. Kim, D. S. & Lee, D. K. Low-temperature catalytic aqueous phase oxidation of microcystin-LR with iron-doped TiO2 pillared clay catalysts. Environ. Technol. (United Kingdom) 0, 1–32 (2020).
7. Pelaez, M. et al. A review on the visible light active titanium dioxide photocatalysts for environmental applications. Appl. Catal. B Environ. 125, 331–349 (2012).
8. MILLS, A., DAVIES, R. H. & WORSLEY, D. ChemInform Abstract: Water Purification by Semiconductor Photocatalysis. ChemInform 25, no-no (2010).
9. Yan, S. et al. Environmentally Safe and Porous MS@TiO2@PPy Monoliths with Superior Visible-Light Photocatalytic Properties for Rapid Oil-Water Separation and Water Purification. ACS Sustain. Chem. Eng. 8, 5347–5359 (2020).
10. Turchi, C. S. & Ollis, D. F. Photocatalytic degradation of organic water contaminants: Mechanisms involving hydroxyl radical attack. J. Catal. 122, 178–192 (1990).
11. Paz, Y. Application of TiO2 photocatalysis for air treatment: Patents' overview. Appl. Catal. B Environ. 99, 448–460 (2010).
12. Tryba, B., Morawski, A. W. & Inagaki, M. Application of TiO2-mounted activated carbon to the removal of phenol from water. Appl. Catal. B Environ. 41, 427–433 (2003).
13. Chen, S., Zhao, M. & Tao, Y. Photocatalytic degradation of organophosphorous pesticides using TiO2 thin film. Chinese J. Catal. 17, 455–458 (1996).
14. Maleki, H. & Bertola, V. TiO2 Nanofilms on Polymeric Substrates for the Photocatalytic Degradation of Methylene Blue. ACS Appl. Nano Mater. 2, 7237–7244 (2019)
15. Haider, A. J., Al-Anbari, R. H., Kadhim, G. R. & Salame, C. T. Exploring potential Environmental applications of TiO2 Nanoparticles. Energy Procedia 119, 332–345 (2017).
16. Bel Hadjltaief, H., Galvez, M. E., Ben Zina, M. & Da Costa, P. TiO2/clay as a heterogeneous catalyst in photocatalytic/photochemical oxidation of anionic reactive blue 19. Arab. J. Chem. 12, 1454–1462 (2019).
17. Loh, K., Gaylarde, C. C. & Shirakawa, M. A. Photocatalytic activity of ZnO and TiO2 'nanoparticles' for use in cement mixes. Constr. Build. Mater. 167, 853–859 (2018).
18. Schneider, J. et al. Understanding TiO2photocatalysis: Mechanisms and materials. Chem. Rev. 114, 9919–9986 (2014).
19. Wu, M. C., Hsiao, K. C., Chang, Y. H. & Kordás, K. Core-Shell Heterostructures of Rutile and Anatase TiO2 Nanofibers for Photocatalytic Solar Energy Conversion. ACS Appl. Nano Mater. 2, 1970–1979 (2019).
20. Espino-Estévez, M. R. et al. Effect of TiO2-Pd and TiO2-Ag on the photocatalytic oxidation of diclofenac, isoproturon and phenol. Chem. Eng. J. 298, 82–95 (2016).
21. Ghori, M. Z. et al. Role of UV Plasmonics in the Photocatalytic Performance of TiO2 Decorated with Aluminum Nanoparticles. ACS Appl. Nano Mater. 1, 3760–3764 (2018).
22. Tom, R. T. et al. Freely dispersible Au@TiO2, Au@ZrO2, Ag@TiO2, and Ag@ZrO2 core-shell nanoparticles: One-step synthesis, characterization, spectroscopy, and optical limiting properties. Langmuir 19, 3439–3445 (2003).
23. Subramanian, V., Wolf, E. E. & Kamat, P. V. Influence of metal/metal ion concentration on the photocatalytic activity of TiO2 - Au composite nanoparticles. Langmuir vol. 19 469–474 (2003).
24. Enache, D. I. et al. Solvent-free oxidation of primary alcohols to aldehydes using Au-Pd/TiO2 catalyst. Science (80-.). 311, 362–365 (2006).
25. Yu, J., Xiong, J., Cheng, B. & Liu, S. Fabrication and characterization of Ag-TiO2 multiphase nanocomposite thin films with enhanced photocatalytic activity. Appl. Catal. B Environ. 60, 211–221 (2005).
26. Li, F. B. & Li, X. Z. The enhancement of photodegradation efficiency using Pt-TiO2 catalyst. Chemosphere 48, 1103–1111 (2002).
27. Hussain, M. et al. Ag–TiO2 nanocomposite for environmental and sensing applications. Mater. Chem. Phys. 181, 194–203 (2016).
28. Sobana, N., Muruganadham, M. & Swaminathan, M. Nano-Ag particles doped TiO2 for efficient photodegradation of Direct azo dyes. J. Mol. Catal. A Chem. 258, 124–132 (2006).
29. Gupta, K., Singh, R. P., Pandey, A. & Pandey, A. Photocatalytic antibacterial performance of TiO2 and Ag-doped TiO2 against S. Aureus. P. Aeruginosa and E. Coli. Beilstein J. Nanotechnol. 4, 345–351 (2013).
30. Akhavan, O. Lasting antibacterial activities of Ag-TiO2/Ag/a-TiO2 nanocomposite thin film photocatalysts under solar light irradiation. J. Colloid Interface Sci. 336, 117–124 (2009).

31. Wilke, C. M., Wunderlich, B., Gaillard, J. F. & Gray, K. A. Synergistic Bacterial Stress Results from Exposure to Nano-Ag and Nano-TiO2 Mixtures under Light in Environmental Media. Environ. Sci. Technol. 52, 3185–3194 (2018).
32. Daghrir, R., Drogui, P. & Robert, D. Modified TiO2 for environmental photocatalytic applications: A review. Ind. Eng. Chem. Res. 52, 3581–3599 (2013)
33. Yadav, S. & Jaiswar, G. Review on Undoped/Doped TiO2 Nanomaterial; Synthesis and Photocatalytic and Antimicrobial Activity. J. Chinese Chem. Soc. 64, 103–116 (2017).
34. Ashkarran, A. A., Aghigh, S. M., Kavianipour, M. & Farahani, N. J. Visible light photo-and bioactivity of Ag/TiO2 nanocomposite with various silver contents. Curr. Appl. Phys. 11, 1048–1055 (2011).
35. Medeiros, E. S., Glenn, G. M., Klamczynski, A. P., Orts, W. J. & Mattoso, L. H. C. Solution blow spinning: A new method to produce micro- and nanofibers from polymer solutions. J. Appl. Polym. Sci. 113, 2322–2330 (2009).
36. Daristotle, J. L., Behrens, A. M., Sandler, A. D. & Kofinas, P. A Review of the Fundamental Principles and Applications of Solution Blow Spinning. ACS Appl. Mater. Interfaces 8, 34951–34963 (2016).
37. Lee, C. G. et al. Porous Electrospun Fibers Embedding TiO2 for Adsorption and Photocatalytic Degradation of Water Pollutants. Environ. Sci. Technol. 52, 4285–4293 (2018).
38. Zhang, J. et al. Preparation of TiO2 Nanofibrous Membranes with Hierarchical Porosity for Efficient Photocatalytic Degradation. J. Phys. Chem. C 122, 8946–8963 (2018).
39. Farias, R. M. D. C., Menezes, R. R., Oliveira, J. E. & De Medeiros, E. S. Production of submicrometric fibers of mullite by solution blow spinning (SBS). Mater. Lett. 149, 47–49 (2015).
40. Oliveira, J. E., Mattoso, L. H. C., Orts, W. J. & Medeiros, E. S. Structural and morphological characterization of micro and nanofibers produced by electrospinning and solution blow spinning: A comparative study. Adv. Mater. Sci. Eng. 2013, (2013).
41. Behrens, A. M. et al. In situ deposition of PLGA nanofibers via solution blow spinning. ACS Macro Lett. 3, 249–254 (2014).
42. Wang, L., Ali, J., Zhang, C., Mailhot, G. & Pan, G. Simultaneously enhanced photocatalytic and antibacterial activities of TiO2/Ag composite nanofibers for wastewater purification. J. Environ. Chem. Eng. 8, 102104 (2020).